Interaction effects on Wannier functions for bosons in an optical lattice

Shaoqi Zhu (朱少奇)[1] and Biao Wu (吴飙)[1,2,3]
[1]*International Center for Quantum Materials, School of Physics, Peking University, Beijing 100871, China*
[2]*Collaborative Innovation Center of Quantum Matter, Beijing 100871, China*
[3]*Wilczek Quantum Center, College of Science, Zhejiang University of Technology, Hangzhou 310014, China*
(Received 13 July 2015; published 30 December 2015)

We have numerically calculated the single-band Wannier functions for interacting Bose gases in optical lattices with a self-consistent approach. We find that the Wannier functions are broadened by repulsive interaction. The tunneling parameter J and the on-site interaction U computed with the broadened Wannier functions are found to change significantly with the number of atoms per site. Our theory can explain the nonuniform atomic clock shift observed in Campbell *et al.*, Science **313**, 649 (2006).

DOI: 10.1103/PhysRevA.92.063637 PACS number(s): 03.75.Lm, 05.30.Jp, 71.15.−m, 73.43.Cd

I. INTRODUCTION

In condensed matter physics, people are often interested in the ground state of the system and its low-energy excitations. This interest allows people to focus only on the lowest band of the system by mapping the system to a lattice model with Wannier functions [1]. The Hubbard model is arguably the most famous of all such lattice models [2]. In addition, Wannier functions are a more natural and better choice than Bloch waves for narrow-band materials in computational physics [3]. There is a lot of freedom to choose a set of Wannier functions as basis and there has been a lot of effort spent finding the best Wannier functions [4]. However, all the discussion is done in the context of single-particle physics. The broadening of Wannier functions by repulsive interactions seems to have never been discussed in traditional condensed matter physics.

The situation began to change with the development of ultracold atomic gases, where the phase transition from superfluid to Mott insulator was observed with a repulsively interacting Bose gas in an optical lattice [5,6]. In the conventional theoretical treatment of such a system, the mapping from the realistic continuous system to the Bose-Hubbard lattice model is done with a single-particle Wannier function [7]. However, due to the simplicity of the periodic potential and small energy scales in the system, it is tempting to think that the broadening of the Wannier function by the on-site repulsive interactions may have significant effects on the system. There have been many theoretical efforts [8–13] that try to describe the interaction effects on the Wannier function.

There is also strong experimental evidence on the broadening of the Wannier function. In the experiment of ^{87}Rb atomic clock in optical lattice [14], nonuniform frequency shifts were observed for different occupation numbers per site. This is clearly due to the broadening of Wannier function by the repulsive atomic interaction.

In Ref. [15], a self-consistent approach is developed to account for the interaction effects on Wannier functions. Using a different set of Wannier functions will result in both a different tunneling parameter J and an on-site interaction U for the lattice model, and thus a different ground state. The self-consistent approach in Ref. [15] uses a general variational principle to choose the set of Wannier functions that minimizes the ground state energy of the lattice model. This method is in spirit the same as the multiconfigurational time-dependent Hartree for bosons theory [16–19].

In this work we use the self-consistent approach in Ref. [15] to compute the interaction effects on Wannier functions for a Bose gas in an optical lattice. We focus on both the superfluid regime and the Mott insulator regime. The broadened Wannier functions are used to calculate the tunneling parameter J and the on-site interaction U in the Bose-Hubbard model. They are found to be significantly affected by the s-wave scattering length, lattice strength, and most importantly the number of atoms per site. At the end, we apply the approach to the experiment in Ref. [14]; our theoretical results match the experimental data very well.

Our paper is organized as follows. In Sec. II, we give a quick review of the self-consistent approach given by Ref. [15]. In Sec. III, we focus on the superfluid regime for a one-dimensional optical lattice; the tunneling parameter J and on-site interaction U are calculated for different lattice depths and interaction strengths. In Sec. IV, we consider the Mott insulator regime; J and U are calculated accordingly. In Sec. V, the theory is applied to the experiment of Ref. [14] and we find good agreement between our theory and the experiment.

II. SELF-CONSISTENT APPROACH FOR WANNIER FUNCTIONS

Here we briefly summarize the self-consistent approach of Ref. [15], which was developed to compute the interaction effects on Wannier functions. We consider a Bose gas where the weak atomic interaction is well described by s-wave scattering. The second quantized Hamiltonian for this kind of system is given by Eq. (1):

$$\hat{H} = \int d\boldsymbol{r}\, \hat{\psi}^\dagger(\boldsymbol{r})\left[-\frac{\hbar^2}{2m}\nabla^2 + V(\boldsymbol{r})\right]\hat{\psi}(\boldsymbol{r}) + \frac{g_0}{2}\int d\boldsymbol{r}[\hat{\psi}^\dagger(\boldsymbol{r})\hat{\psi}^\dagger(\boldsymbol{r})\psi(\boldsymbol{r})\psi(\boldsymbol{r})], \quad (1)$$

where m is the atomic mass and $V(\boldsymbol{r})$ describes an optical lattice. And $g_0 = 4\pi\hbar^2 a_s/m$ is the interaction strength related to the s-wave scattering length a_s. The single-band approximation expands the boson field operator $\psi(\boldsymbol{r})$ as shown by

Eq. (2):

$$\hat{\psi}(\boldsymbol{r}) = \sum_j \hat{a}_j W_j(\boldsymbol{r}), \tag{2}$$

where $W_j(\boldsymbol{r}) = W(\boldsymbol{r} - \boldsymbol{r}_j)$ is the Wannier function at site j and $\hat{a}_j$ is the associated annihilation operator. The ground state $|G_t\rangle$ in the single-band approximation can be generally written as $|G_t\rangle = F(\hat{a}_j^\dagger)|\text{vaccum}\rangle$, where F is the function to be found by solving the resulting lattice model. The ground state energy $E_G = \langle G_t|\hat{H}|G_t\rangle$ certainly changes with the choice of Wannier function $W_j(\boldsymbol{r})$. The best Wannier function is the one that minimizes the single-band ground state energy E_G. Mathematically, the minimization is achieved by using the variation given by Eq. (3):

$$\frac{\delta E_G}{\delta W^*(\boldsymbol{r})} - \frac{\delta \sum_j \mu_j h_j}{\delta W^*(\boldsymbol{r})} = 0, \tag{3}$$

with the orthonormal constraints given by Eq. (4):

$$h_j = \int d\boldsymbol{r}\, W^*(\boldsymbol{r}) W(\boldsymbol{r} - \boldsymbol{r}_j) = \delta_{0,j}. \tag{4}$$

μ_j's are the usual Lagrangian multipliers. With straightforward computation, a nonlinear equation [Eq. (5)] was obtained for the interacting Wannier functions [15]:

$$\begin{aligned}
&\sum_j \mu_j W(\boldsymbol{r} - \boldsymbol{r}_j) \\
&= \sum_{j_1, j_2} \langle \hat{a}_{j_1}^\dagger \hat{a}_{j_2} \rangle H_0 W(\boldsymbol{r} + \boldsymbol{r}_{j_1} - \boldsymbol{r}_{j_2}) \\
&\quad + g_0 \sum_{j_1 j_2}^{j_3 j_4} \langle \hat{a}_{j_1}^\dagger \hat{a}_{j_2}^\dagger \hat{a}_{j_3} \hat{a}_{j_4} \rangle W^*(\boldsymbol{r} + \boldsymbol{r}_{j_2} - \boldsymbol{r}_{j_1}) \\
&\quad \times W(\boldsymbol{r} + \boldsymbol{r}_{j_2} - \boldsymbol{r}_{j_4}) W(\boldsymbol{r} + \boldsymbol{r}_{j_2} - \boldsymbol{r}_{j_3}),
\end{aligned} \tag{5}$$

where $\langle \cdot \rangle$ represents averaging over the ground state of the system and $H_0 = -\frac{\hbar^2}{2m}\nabla^2 + V(\boldsymbol{r})$. The ground state is found with the Bose-Hubbard model shown by Eq. (6):

$$\hat{H}_h = -J \sum_{\langle ij \rangle} \hat{a}_i^\dagger \hat{a}_j + \frac{U}{2} \sum_i \hat{a}_i^\dagger \hat{a}_i (\hat{a}_i^\dagger \hat{a}_i - 1), \tag{6}$$

where

$$J = -\int d\boldsymbol{r}\, W^*(\boldsymbol{r} - \boldsymbol{r}_j) H_0 W(\boldsymbol{r} - \boldsymbol{r}_{j-1}) \tag{7}$$

and

$$U = g_0 \int d\boldsymbol{r} |W(\boldsymbol{r})|^4. \tag{8}$$

Euations (5) and (6) need to be solved self-consistently together to find the best Wannier function $W(\boldsymbol{r})$.

In this work, except in Sec. V where we try to explain a three-dimensional experiment, we focus on one-dimensional optical lattice $V(x) = V_0 \sin^2(k_L x)$, where V_0 is the optical lattice strength and k_L is the wave vector of the laser generating the optical lattice. In our calculation, g_0 is in units of $E_r \pi^3 / k_L^3$, where $E_r = \hbar^2 k_L^2 / 2m$ is the recoil energy. In the case of ^{87}Rb , $a_s = 5.32$ nm and $g_0 \approx 0.12 E_r \pi^3 / k_L^3$.

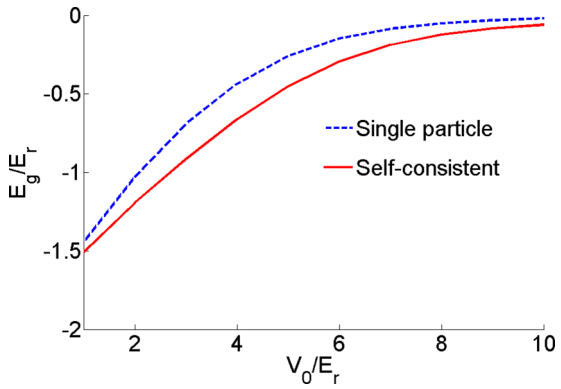

FIG. 1. (Color online) The ground state energies of a six-site Bose-Hubbard model computed with the usual single-particle method (blue line) and our self-consistent method (red line). The mean particle number per site $n_0 = 1$. $g_0 = 1 E_r \pi^3 / k_L^3$.

We first consider an example, which is a one-dimensional six-site Bose-Hubbard model with one atom per site. For this simple case, we can find its ground state with exact diagnalization [20]. We use two different ways to compute J and U in the model: (1) with the single-particle Wannier function and (2) with the interacting Wannier function obtained self-consistently with Eqs. (5) and (6). Figure 1 shows a comparison of the ground state energy calculated by these two methods for the Bose-Hubbard model. The energy computed with the self-consistent method is indeed lower. Figure 2 shows one Wannier function that we obtained with the self-consistent method, which is apparently broadened by the interaction. These broadened Wannier functions can influence the tunneling parameter J and the on-site interaction U in the single-band Bose-Hubbard model. In the following two sections, we shall compute the broadened Wannier function in both the superfluid regime and Mott regime for one-dimensional systems.

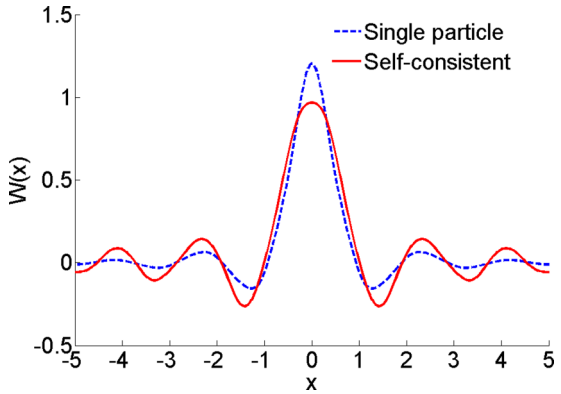

FIG. 2. (Color online) Comparison between a single-particle Wannier function (blue line) and its corresponding broadened Wannier function (red line) obtained by the self-consistent method. x is in units of $\lambda/2$, where $\lambda = 2\pi/k_L$. In this calculation, the lattice model has ten sites with $n_0 = 7$, $V_0 = E_r$, and $g_0 = 1 E_r \pi^3 / k_L^3$. The on-site interaction is $U \approx 0.33 E_r$, which is smaller than the band gap.

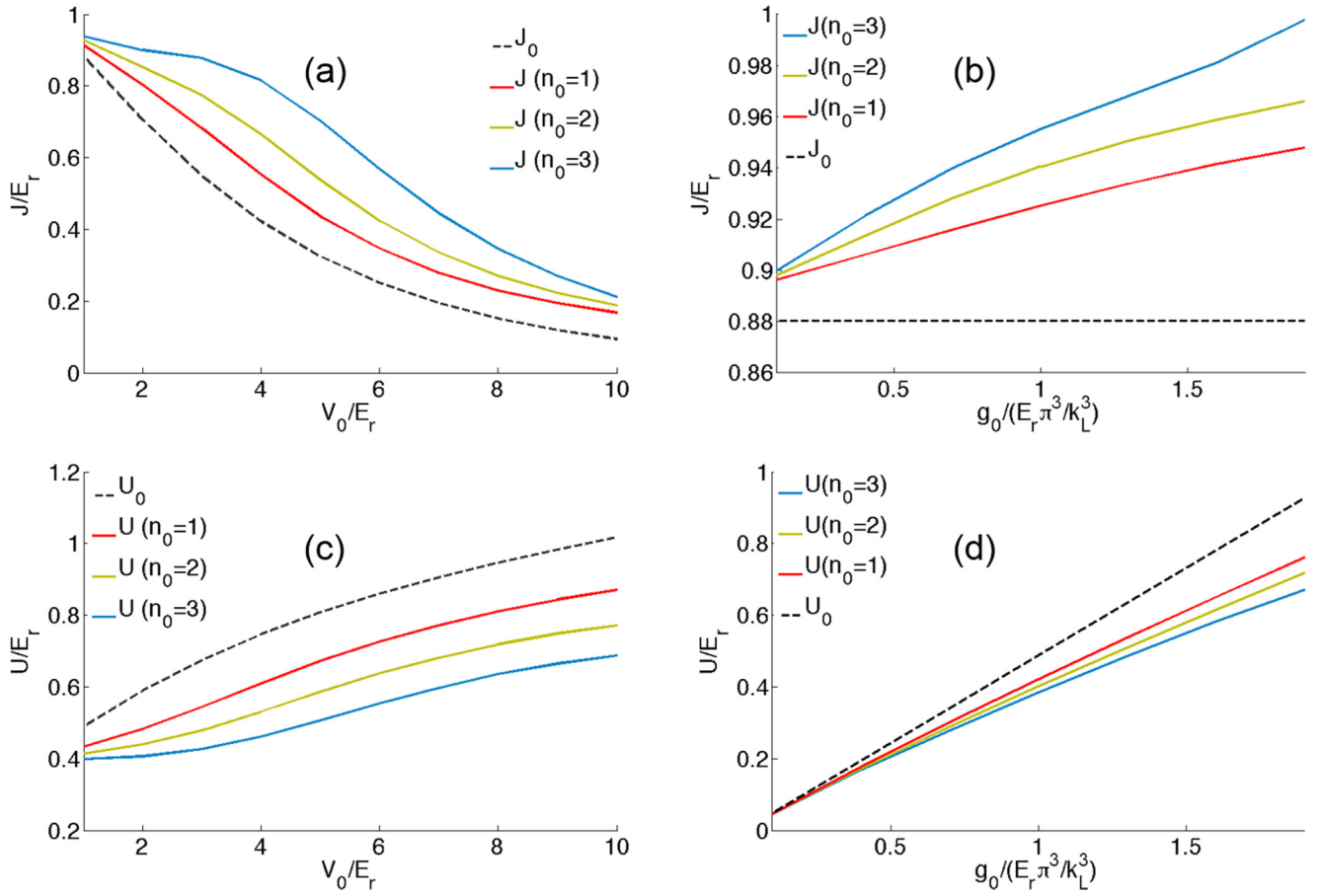

FIG. 3. (Color online) Superfluid regime with ten lattice sites. (a) Change of tunneling parameter J with potential depth for different n_0. $g_0 = E_r\pi^3/k_L^3$; (b) change of J with interaction strength for different n_0. $V_0 = E_r$; (c) change of on-site interaction U with potential depth for different n_0. $g_0 = E_r\pi^3/k_L^3$; (d) change of U with interaction strength for different n_0. $V_0 = E_r$.

III. SUPERFLUID REGIME

In the superfluid regime all the particles condense into the ground state of the system which is a Bloch state. Therefore, it is more convenient to use the Bloch basis in which the nonlinear equations in Eq. (5) become Eq. (9) [15]:

$$\tilde{v}_{\boldsymbol{k}}\psi_{\boldsymbol{k}}(\boldsymbol{r}) = H_0\psi_{\boldsymbol{k}}(\boldsymbol{r}) + g_0 \sum_{\langle \boldsymbol{k}_1\boldsymbol{k}\boldsymbol{k}_3\boldsymbol{k}_4\rangle} P_{\boldsymbol{k}_1\boldsymbol{k}\boldsymbol{k}_3\boldsymbol{k}_4}\psi^*_{\boldsymbol{k}_1}(\boldsymbol{r})\psi_{\boldsymbol{k}_3}(\boldsymbol{r})\psi_{\boldsymbol{k}_4}(\boldsymbol{r}), \quad (9)$$

where $P_{\boldsymbol{k}_1\boldsymbol{k}\boldsymbol{k}_3\boldsymbol{k}_4} = \langle \hat{b}^\dagger_{\boldsymbol{k}_1}\hat{b}^\dagger_{\boldsymbol{k}}\hat{b}_{\boldsymbol{k}_3}\hat{b}_{\boldsymbol{k}_4}\rangle / \langle \hat{b}^\dagger_{\boldsymbol{k}}\hat{b}_{\boldsymbol{k}}\rangle$ with $\hat{b}_{\boldsymbol{k}} = \frac{1}{\sqrt{N}}\sum_j \hat{a}_n e^{-i\boldsymbol{k}\cdot\boldsymbol{r}_j}$. In the superfluid phase, the Bogoliubov mean-field theory [21] can be used to determine and compute $P_{\boldsymbol{k}_1\boldsymbol{k}\boldsymbol{k}_3\boldsymbol{k}_4}$ and other coefficients in Eq. (9) [15]. There is no deed to solve the lattice model in Eq. (6).

In our computation, we expand the Bloch function $\psi_{\boldsymbol{k}}$ with plane waves according to Eq. (10):

$$\psi_{\boldsymbol{k}}(\boldsymbol{r}) = \frac{1}{\sqrt{N\Omega}}\sum_{\boldsymbol{K}} a(\boldsymbol{k}+\boldsymbol{K})e^{i(\boldsymbol{k}+\boldsymbol{K})\cdot\boldsymbol{r}}, \quad (10)$$

where Ω is the volume of a cell and N is the number of cells. After plugging Eq. (10) into Eq. (9), we obtain a set of nonlinear equations for $a(\boldsymbol{k})$'s. We solve these nonlinear equations numerically and then construct the Wannier functions by carefully choosing the phases of all the Bloch functions with Kohn's method [22].

Figure 3 shows how J and U change with lattice strength V_0 and interaction parameter g_0 for different n_0, the mean particle number per site. It is apparent that the different curves for different n_0's have roughly the same overall trend but they do shift from each other significantly. For J, as n_0 increases, the curves for J shift upwards and the curves for U shift downwards, meaning J increases with n_0 while U decreases. The increase of J and decrease of U with n_0 is due to the broadening of Wannier functions. In the range shown in Fig. 3, J can change up to 100% at $n_0 = 3$ compared to that of a single-particle result, while U can change up to 30%.

IV. MOTT-INSULATOR REGIME

In the deep Mott-insulator regime the ground state can be approximated with $|n_0,n_0,\ldots,n_0\rangle$. As a result, the nonlinear equations for Wannier function in Eq. (5) are simplified to Eq. (11):

$$\sum_j \frac{\mu_j}{N_0}W(\boldsymbol{r}-\boldsymbol{r}_j) = H_0W(\boldsymbol{r}) + g_0(n_0-1)|W(\boldsymbol{r})|^2W(\boldsymbol{r}) + 2g_0n_0\sum_{\boldsymbol{r}_j\neq 0}|W(\boldsymbol{r}-\boldsymbol{r}_j)|^2W(\boldsymbol{r}). \quad (11)$$

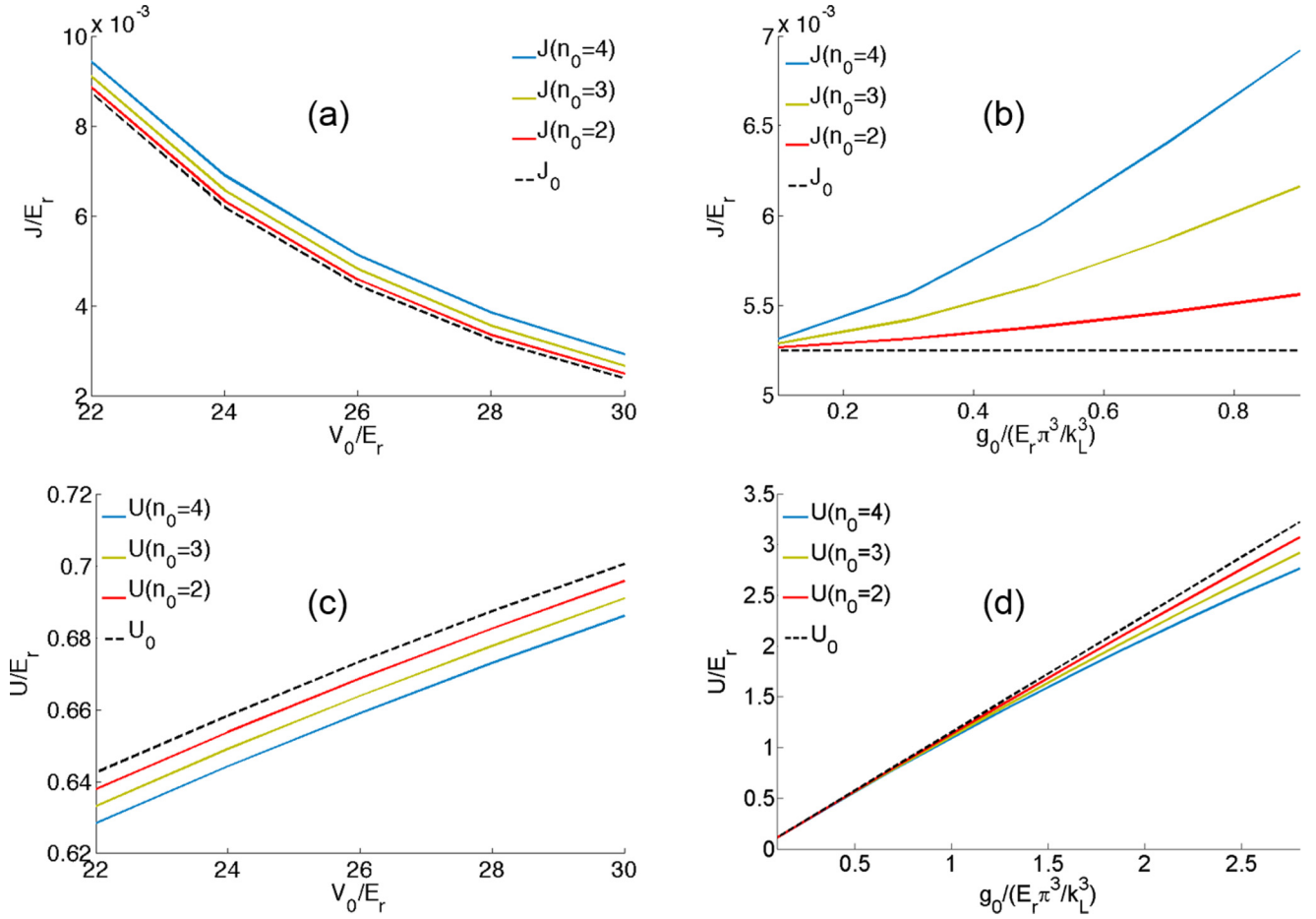

FIG. 4. (Color online) Mott-insulator regime with ten lattice sites. (a) Change of tunneling parameter J with potential depth for different n_0. $g_0 = 0.5E_r\pi^3/k_L^3$; (b) change of J with interaction strength for different n_0. $V_0 = 25E_r$; (c) change of on-site interaction U with potential depth for different n_0. $g_0 = 0.5E_r\pi^3/k_L^3$; (d) change of U with interaction strength for different n_0. $V_0 = 25E_r$.

In our numerical computation, we expand the Wannier function in terms of single-particle Wannier functions on the same site and its nearest neighbors according to Eq. (12):

$$W(\boldsymbol{r}-\boldsymbol{r}_j) = \sum_{n=1}^{M}[c_n w_n(\boldsymbol{r}-\boldsymbol{r}_{j-1}) + b_n w_n(\boldsymbol{r}-\boldsymbol{r}_j) + c_n w_n(\boldsymbol{r}-\boldsymbol{r}_{j+1})], \quad (12)$$

where $w_n(\boldsymbol{r}-\boldsymbol{r}_j)$ is the single-particle Wannier function for Bloch band n at site j. After conducting a convergence test, we set $M = 3$. We solve Eq. (11) numerically to find the interaction-broadened Wannier functions, and then compute J and U. The results are shown in Fig. 4. It is clear that the general trends how J and U change with g_0 and V_0 in the Mott regime are similar to the ones in the superfluid regime. However, there are differences. Specifically, as shown in Figs. 4(a) and 4(c), the change of both J and U with n_0 has little dependence on the lattice depth V_0. We notice from Fig. 4 that with our self-consistent approach J can change up to 32% at $n_0 = 4$ compared to that of single-particle Wannier function, while U can change up to 14%.

V. NONUNIFORM ATOMIC CLOCK SHIFT

Atomic clock frequency can shift due to the collision of atoms. In an experiment reported by Ref. [14], the atomic clock shift of ^{87}Rb was measured. In the experiment, a ^{87}Rb Bose-Einstein condensate was prepared in the $|F = 1, m_f = -1\rangle$ state and loaded into a three-dimensional optical lattice. With the increase of the lattice depth, the system changed from the superfluid phase to a Mott-insulator (MI) phase. Due to the trapping potential the atomic gases was separated into MI shells, each of which has a different occupation number n_0. Radio waves were used to excite atoms in the $F = 1$ state to $F = 2$ state. In different hyperfine states, the scattering lengths between atoms are different. Therefore, the atoms transferred to the $F = 2$ state have a slightly different mean-field energy; this can cause a clock frequency shift, which is shown by Eq. (13) [21,23,24]:

$$\delta\nu = \frac{U}{h}(a_{21} - a_{11})/a_{11}, \quad (13)$$

where a_{11} and a_{22} are scattering lengths for atoms in the $F = 1$ and $F = 2$ states, respectively, and a_{12} is the scattering length between an atom in the $F = 1$ state and an atom in the $F = 2$ state. If the on-site interaction U is calculated with

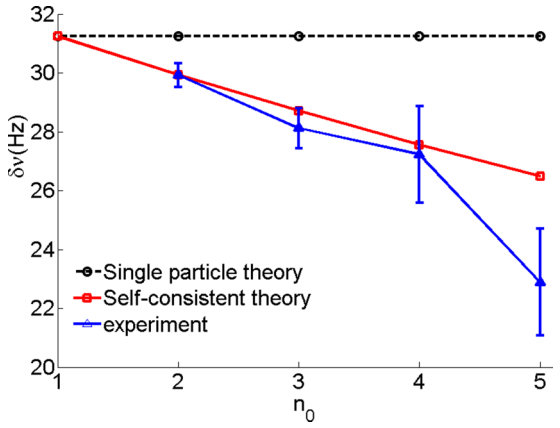

FIG. 5. (Color online) Clock shifts for different number of atoms per site n_0. The experiment data for the trhe-dimensional lattice depth of $V_0 = 35E_r$ are from Ref. [14] and provided courtesy of Gretchen Campbell.

single-particle Wannier functions, this clock shift is independent of n_0, the number of atoms per site. However, it was observed in the experiment that the clock shift decreases with n_0 as shown in Fig. 5.

In our view, this decrease of clock frequency shift in Fig. 5 is caused by the broadening of Wannier function: when n_0 increases, the Wannier function becomes broader and U decreases as shown in Figs. 4(c) and 4(d); consequently, the clock shift decreases. With our self-consistent method, we calculated the interacting Wannier functions for different n_0's in the Mott-insulator regime achieved in Ref. [14]. We then computed U and the clock shift $\delta\nu$; the results are compared to the experimental results in Fig. 5. There is very good agreement.

VI. CONCLUSION

With a self-consistent theory developed earlier [15], we have computed the effect of interactions on single-band Wannier functions. We considered both the superfluid regime and the Mott regime. We found that as the result of broadening of the Wannier function through interactions, the tunneling parameter J and U can change significantly. Our theory was applied to a clock shift experiment; very good agreement was found between our theoretical results and experimental results. The regime near the transition from superfluid to Mott insulator is not studied in this work and will be investigated in the future.

ACKNOWLEDGMENTS

We thank Qizhong Zhu for helpful discussions. We are grateful to Gretchen Campbell for providing the original experiment data in Ref. [14]. This work is supported by the NBRP of China (Grants No. 2013CB921903 and No. 2012CB921300) and the NSF of China (Grants No. 11274024, No. 11334001, and No. 11429402).

[1] G. H. Wannier, Phys. Rev. **52**, 191 (1937).
[2] N. W. Ashcroft and N. D. Mermin, *Solid State Phyics* (Sanders, Philadelphia, 1976).
[3] N. Marzari and D. Vanderbilt, Phys. Rev. B **56**, 12847 (1997).
[4] W. Kohn, Phys. Rev. B **7**, 4388 (1973).
[5] M. Greiner, O. Mandel, T. W. Hansch, and I. Bloch, Nature (London) **415**, 39 (2002).
[6] I. Bloch, J. Dalibard, and W. Zwerger, Rev. Mod. Phys. **80**, 885 (2008).
[7] D. Jaksch, C. Bruder, J. I. Cirac, C. W. Gardiner, and P. Zoller, Phys. Rev. Lett. **81**, 3108 (1998).
[8] J. B. Li, Y. Yu, A. M. Dudarev, and Q. Niu, New J. Phys. **8**, 154 (2006).
[9] Z. X. Liang, B. B. Hu, and B. Wu, arXiv:0903.4058.
[10] P. I. Schneider, S. Grishkevich, and A. Saenz, Phys. Rev. A **80**, 013404 (2009).
[11] D. Masiello, S. B. McKagan, and W. P. Reinhardt, Phys. Rev. A **72**, 063624 (2005).
[12] V. Yukalov, Laser Phys. **19**, 1 (2009).
[13] D. S. Luhmann, O. Jurgensen, and K. Sengstock, New J. Phys. **14**, 033021 (2012).
[14] G. K. Campbell, J. Mun, M. Boyd, P. Medley, A. E. Leanhardt, L. G. Marcassa, D. E. Pritchard, and W. Ketterle, Science **313**, 649 (2006).
[15] B. Wu, Y. Xu, L. Dong, and J. R. Shi, Chin. Phys. Lett. **29**, 083701 (2012).
[16] O. E. Alon, A. I. Streltsov, and L. S. Cederbaum, Phys. Rev. Lett. **95**, 030405 (2005).
[17] A. I. Streltsov, O. E. Alon, and L. S. Cederbaum, Phys. Rev. A **73**, 063626 (2006).
[18] O. E. Alon, A. I. Streltsov, and L. S. Cederbaum, Phys. Rev. A **77**, 033613 (2008).
[19] K. Sakmann, A. I. Streltsov, O. E. Alon, and L. S. Cederbaum, New J. Phys. **13**, 043003 (2011).
[20] J. M. Zhang and R. X. Dong, Eur. J. Phys. **31**, 591 (2010).
[21] C. J. Pethick and H. Smith, *Bose-Einstein Condensation in Dilute Gases*, 2nd ed. (Cambridge University Press, Cambridge, UK, 2008).
[22] W. Kohn, Phys. Rev. **115**, 809 (1959).
[23] D. M. Harber, H. J. Lewandowski, J. M. McGuirk, and E. A. Cornell, Phys. Rev. A **66**, 053616 (2002).
[24] G. Baym and C. J. Pethick, Phys. Rev. Lett. **76**, 6 (1996).